Published in final edited form as:
Vet Ophthalmol. 2010 January ; 13(1): 37–42. doi:10.1111/j.1463-5224.2009.00755.x.

Isolation and cultivation of equine corneal keratocytes, fibroblasts and myofibroblasts

Dylan G. Buss[*], **Elizabeth A. Giuliano**[*], **Ajay Sharma**[†,‡], and **Rajiv R. Mohan**[*,†,‡]

[*] College of Veterinary Medicine, University of Missouri, Columbia, MO, USA

[†] Mason Eye Institute, University of Missouri, Columbia, MO, USA

[‡] Ophthalmology Research Services, Harry S. Truman Memorial Veterans Hospital, Columbia, MO, USA

Abstract

Objective—To establish an *in vitro* model for the investigation of equine corneal wound healing. To accomplish this goal, a protocol to isolate and culture equine corneal keratocytes, fibroblasts and myofibroblasts was developed.

Animal material—Equine corneal buttons were aseptically harvested from healthy research horses undergoing humane euthanasia for reasons unrelated to this study. Slit-lamp biomicroscopy was performed prior to euthanasia by a board-certified veterinary ophthalmologist to ensure that all samples were harvested from horses free of anterior segment disease.

Procedure—Equine corneal stroma was isolated using mechanical techniques and stromal sub-sections were then cultured. Customized media at different culture conditions was used to promote growth and differentiation of corneal stromal cells into keratocytes, fibroblasts and myofibroblasts.

Results—Cell culture techniques were successfully used to establish a method for the isolation and culture of equine corneal keratocytes, fibroblasts and myofibroblasts. Immunohistochemical staining for alpha-smooth muscle and F-actin was used to definitively differentiate the three cell types.

Conclusion—Equine corneal stromal keratocytes, fibroblasts and myofibroblasts can be predictably isolated and cultured *in vitro* using this protocol.

Keywords

cornea; corneal wound healing; equine; fibroblasts; keratocytes; myofibroblasts

INTRODUCTION

Corneal transparency is essential for vision. The cornea's unique structural anatomy acts as the eye's first refractive media, accounting for up to 75% of the total refractive state in terrestrial animals.[1,2] Therefore, any ocular disease that affects the cornea's transparency affects vision. Corneal disorders are one of the most significant causes of vision loss in the horse. Corneal wound healing resulting from inflammation, infection, ocular trauma, autoimmune disease or neoplasia, affects corneal transparency, and therefore vision. When vision is compromised, a horse's performance is impaired, and treatment is frequently costly and time consuming.

Address communications to: Dr. R. R Mohan, Tel.: 573 884 1449, Fax: 573 884 6551, mohanr@health.missouri.edu.

The equine cornea ranges between 0.8 and 1.0 mm in thickness.[1] It is comprised of four basic layers: (i) epithelium consisting of 8–10 cell layers (~60 μm), (ii) stroma (~700 μm), (iii) Descemet's membrane (14–21 μm) and (iv) endothelium (7 μm).[1] The stroma in the cornea is composed of collagen bundles (85–90%), extracellular matrix and keratocytes, and constitutes 90% of the cornea's overall thickness. [2] Gap junctions between normal corneal keratocytes and fibroblasts enable cellular interactions. Corneal trauma resulting in epithelial breakdown leads to stromal cell activation, protein synthesis, cytokine release, loss of cell to cell contact, and culminates in the transformation of local keratocytes and fibroblasts to myofibroblasts.[2, 3] Numerous cytokines are involved in this process; however, tissue growth factor beta (TGF-β) has been demonstrated to play a key role in the transdifferentiation of keratocyte to fibroblasts and myofibroblasts.[4] The contractile property of myofibroblasts is due to the intracellular F-actin microfilament fibers comprising of alpha-smooth muscle actin (α-SMA), myosin, α-actinin, and associated surface membrane receptors such as $\alpha_5\beta_1$-integrin receptor, and fibronectin (FN). Contrary to myofibroblasts, quiescent keratocytes are flat interconnected stellate cells with contractile proteins localized to the cell cortex.[2] The process of wound contracture and corneal healing relies on the presence of myofibroblasts. With the completion of corneal wound healing, a reduction in myofibroblast number normally occurs. When myofibroblasts fail to regress in number, abnormal wound healing and corneal fibrosis result.[3]

Development of an *in vitro* model of equine corneal stromal cells is a critical first step in furthering our understanding of corneal wound healing in this species. Nonetheless, it is important to note that corneal wound healing is a complex process and may require a battery of *in vitro* models. The goal of this study was to reliably isolate pure cultures of equine corneal keratocytes, fibroblasts and myofibroblasts from healthy equine corneal buttons. These cultures can be used to study the effects of topical pharmaceuticals, growth factors, and bacterial toxins on the specific cells.

MATERIALS AND METHODS

Corneal biopsy collection

Full-thickness 6-mm axial corneal buttons were aseptically harvested from five healthy research horses undergoing humane euthanasia for reasons unrelated to this study. Slit-lamp biomicroscopy was performed prior to euthanasia to ensure that all samples were harvested from horses free of anterior segment disease.

Isolation of equine corneal fibroblasts primary cultures

Corneal buttons were washed with minimum essential medium (MEM; Invitrogen, Carlsbad, CA, USA) and the epithelium and endothelium was removed by gentle scraping using a #15 Bard Parker (BD, Franklin Lakes, NJ, USA) scalpel blade. Corneal stroma was sub-sectioned and placed in tissue culture plates containing Dulbecco's modified Eagle's medium (DMEM; Invitrogen) containing 10% fetal bovine serum to obtain equine corneal fibroblasts (ECF). ECF were then incubated in a humidified 5% CO_2 incubator (HERA-cell, Thermo Scientific, Waltham, MA, USA) at 37 °C. In approximately 3–5 days, fibroblasts began migrating from the stromal sub-sections. Once the primary culture reached 90% confluence, the stromal sub-sections were manually removed using rat-toothed forceps and discarded. The confluent cells were trypsinised and re-plated on 60 mm tissue plates in customized media at different culture conditions to promote growth and differentiation of corneal stromal fibroblasts into keratocytes and myofibroblasts.

Isolation of equine corneal keratocytes, fibroblasts and myofibroblasts

Monocultures of corneal keratocytes, fibroblasts and myofibroblasts were selectively induced from the primary cultures generated from corneal explants by altering media or cell seeding conditions. Specifically, a concentration of 50 000 cells per 60 mm plate in serum-free MEM provided equine corneal keratocyte cultures. Equine fibroblast cultures were selectively produced by seeding 50 000 cells per 12-well plate in MEM medium supplemented with 10% fetal bovine serum. Myofibroblast cultures were induced from ECF seeding 10 000 fibroblasts per 60 mm plate in MEM medium supplemented with 10% fetal bovine serum or serum-free MEM medium containing 1 ng/mL transforming growth factors beta 1 (TGFβ1). The culture parameters (temperature, humidity, CO_2, etc.) remained the same as those described for obtaining primary ECF cultures.

Immunohistochemistry for corneal stromal cell markers

Immunohistochemistry was used to confirm the presence of equine corneal keratocytes, fibroblasts and myofibroblasts. Immunofluorescent staining for F-actin and α-SMA was performed using mouse monoclonal antibody for α-SMA (Invitrogen) and phalloidin (Invitrogen). Cultured ECF's were washed with PBS and incubated at room temperature with monoclonal antibody for either F-actin or α-SMA at a 1:200 dilution in 1× PBS for 90 min and with secondary antibody Alexa 488 goat anti-mouse IgG (Invitrogen) at a dilution of 1:500 for 1 h. Cells were mounted with Vectashield containing DAPI (Vector Laboratories, Inc., Burlingame, CA, USA) to allow visualization of nuclei. Irrelevant isotype-matched primary antibody, secondary antibody alone, and tissue sections from naïve eyes were used as negative controls. Immunostained cultures were examined and photographed with Leica fluorescent microscope (Leica, Wetzlar, Germany) equipped with a CCD digital camera (SpotCam RT KE, Diagnostic Instruments Inc., Sterling Heights, MI, USA).

Cellular morphology and viability

The cellular phenotype of cultures was monitored with a phase-contrast microscope (Leica DMIL) equipped with an imaging system (Leica DFC290). The cultures were photographed at different time intervals to record cellular morphology. Cellular viability of all cell types was examined using trypan blue assay. Briefly, trypsinised cells were mixed with equal amounts of cell biology grade 0.4% trypan blue solution (Invitrogen). Dead cells with ruptured membranes stained blue and live white cells were counted using Neubauer's chamber. Data were expressed as percentage of dead cells vs. total cell count.

Quantification using real-time PCR

Total RNA from the cells was extracted using RNeasy kit (Qiagen Inc., Valencia, CA, USA) and was reverse transcribed to cDNA following vendor's instructions (Promega, Madison, WI, USA). Real-time PCR was performed using iQ5 real-time PCR Detection System (Bio-Rad Laboratories, Hercules, CA, USA). Fifty micro liters reaction mixture containing 2 μL cDNA (250 ng), 2 μL forward (200 nM); 2 μL reverse primer (200 nM) and 25 μL 2× iQ SYBR green super mix (Bio-Rad Laboratories) were run at universal cycle (95 °C for 3 min, 40 cycles of 95 °C for 30 s followed by 60 °C for 60 s) following the vendor's instructions. For α-SMA, forward primer sequence TGGGTGACGAAGCACAGAGC and reverse primer sequence CTTCAGGGGCAACACGAAGC were used. Beta actin forward primer (CGGCTACAGCTTCACCACCA) and reverse primer (CGGGCAGCTCGTAGCTCTTC) were used as a house keeping gene. The threshold cycle (Ct) was used to detect the increase in the signal associated with an exponential growth of PCR product during the log-linear phase. The relative expression was calculated using the following formula, $2^{-\Delta\Delta}$Ct. The ΔCt validation experiments showed similar amplification efficiency for all templates used (difference between linear slopes for all templates <0.1). Results were expressed as mean ±

SEM. Statistical analysis was performed using an unpaired student *t*-test in which $P < 0.05$ was considered significant.

Image and statistical analysis

Statistical analysis was performed using two-way analysis of variance (ANOVA) followed by Bonferroni multiple comparisons test for viability and other assays. The real-time PCR data results were analyzed using one-way ANOVA followed by Tukey's multiple comparison tests. A '*P*'-value <0.05 was considered significant. The immunocytochemistry data was analyzed using image J 1.38 X image analysis software (NIH, Bethesda, MD, USA).

RESULTS

Light microscopic examination

Equine corneal fibroblasts, keratocytes and myofibroblasts were cultured using the methodology described above. The cells grown under serum-free conditions had a similar morphological appearance as keratocytes *in situ*, demonstrating long, broad, stellate cytoplasmic morphology with multiple interconnected cellular processes (Fig. 1a).[5] On the other hand cells grown in 10% serum supplemented medium demonstrated classic spindle shaped fibroblast morphology (Fig. 1b). Contrary to these observations, equine stromal cell cultures grown in serum-free medium containing TGFβ1 (1 ng/mL) were larger in size exhibiting the typical corneal myofibroblastic phenotype (Fig. 1c).[5] Keratocytes had the lowest proliferation rates typical of that observed *in vivo* in equine cornea while corneal fibroblasts had the highest proliferation rates reaching confluence in 3–4 days. Keratocyte transdifferentiation to myofibroblasts under serum-free condition in the presence of TGFβ1 (1 ng/mL) was gradual from day 3 to 10. At day-10, over 90% ($P < 0.01$) of cells in the culture grown in the presence of TGFβ1 (1 ng/mL) demonstrated myofibroblastic phenotype whereas only 4–8% myofibroblasts were observed in the cultures grown in serum-containing (10%) medium. Keratocytes and myofibroblasts achieved confluence in 10–12 days under serum-free conditions.

Immunocytochemical evaluation

Immunocytochemistry examinations of phalloidin (F-actin) and α-SMA staining patterns were unique to each of the three examined equine corneal cell phenotypes. The keratocytes appeared as a homogenous cell population composed of long, flat, interconnected, stellate cells with F-actin staining localized to the cell cortex and occasional or no staining of discernable fibers (Fig. 2a). Cells in cultures fed with 10% serum-containing medium were spindle shaped and long showing typical fibroblastic phenotype with an intracellular staining for F-actin in microfilament bundles (Fig. 2b). Myofibroblasts were larger, wider and broader with a substantial increase in the contractile apparatus that stained distinctively and strong for F-actin (Fig. 2c). Figure 3 shows immunohistochemistry for α-SMA for the equine corneal cell phenotypes. Keratocytes did not show positive α-SMA staining (Fig. 3a), fibroblasts demonstrated sparse α-SMA staining in few cells (Fig. 3b) and myofibroblasts revealed extremely high α-SMA staining in all the cells ($P < 0.01$), (Fig. 3c). The sparse α-SMA staining observed in fibroblasts could be attributable to myofibroblast contamination. Nonetheless, it is important to mention that even though few fibroblast cells (4–8%) in culture showed high α-SMA staining they still retained a predominantly fibroblast-like phenotype. It is conceivable that as the populations of cells shift from one phenotype to another under specific conditions they may show sparse populations of their previous phenotypes. Senescence in any phenotype was not observed during this study.

Viability evaluation

The cellular viability of all three phenotypes was >98% ($P < 0.01$) as demonstrated by a lack of positive trypan blue staining. These results suggest that the medium composition and culture conditions defined for the equine corneal keratocyte, fibroblast and myofibroblast cultures were optimal for growing and maintaining these cultures for a long time. The trypan assay data has not been included.

Quantification of real-time PCR

The relative expression of α-SMA quantified using real-time PCR for the three phenotypes has been shown in Fig. 4. No α-SMA expression was detected in keratocytes whereas myofibroblasts showed highest α-SMA levels. The quantity of α-SMA mRNA was found to be >1.5-folds in myofibroblasts compared to keratocytes or fibroblasts ($P < 0.01$). These results were consistent with the findings of α-SMA immunocytochemistry.

DISCUSSION

Corneal disease is one of the most common ocular disorders of horses worldwide.[6,7] Historically in veterinary ophthalmology, treatment has focused primarily on globe preservation and restoration of ocular comfort and lesser on the restoration of normal vision, particularly in cases of severe keratitis. Treatment strategies aiming specifically at the reduction of corneal scarring are grossly lacking in the horse. Corneal scarring or 'haze' as it is referred to in physician ophthalmology, has been the topic of numerous studies. In hopes to reduce haze in patients who undergo photorefractive laser eye surgery (PRK, LASIK etc.), experimentation in mouse, rabbit and human corneas have been completed. Mitomycin C has been proven to be effective at reducing haze.[8–13] Recently, trichostatin A has proved effective in blocking the effect of TGFβ1 and thereby reducing corneal haze.[14] Gene therapy is a new treatment modality which is demonstrating promise. The decorin gene, which is a natural inhibitor of TGFβ1-3, successfully introduced into rabbit corneal fibroblasts with adeno-associated virus (AAV) vector blocked the fibrotic effects of TGFβ1, thereby reducing corneal fibrosis *in vitro*.[15] It might be a better approach to find agents that prevent rather than treat corneal scarring.

An *in vitro* model is therefore highly desired for studying wound healing events in the equine cornea and testing the efficacy of potential therapeutic agents for the prevention and treatment of corneal scarring in horses. To the best of authors' knowledge there have been no previous reports of an *in vitro* equine corneal wound healing model. Haber *et al.*, examined the effects of growth factors (EGF, PDGF-BB and TGF-beta 1) on cultured equine epithelial cells and keratocytes;[16,17] however, our investigation differs in that our goal was to successfully establish three separate, reproducible cell lines from equine stroma only. This study reports optimal conditions for growing equine corneal keratocytes, fibroblasts and myofibroblasts that serve as a model for studying various aspects of equine corneal wound healing. The proliferation rates, morphology, distribution of F-actin and α-SMA marker proteins were similar to those results published for keratocytes, fibroblasts and myofibroblasts from other species (canine and rabbit).[16–23] We were able to establish the growth of ECF by culturing corneal stromal sub-sections at cellular density of 50 000 cells/12-well plate in the presence of serum. The keratocyte phenotype was induced by culturing the ECF under serum-free conditions whereas equine corneal myofibroblast cultures were obtained by plating the ECF at a lower density (10 000 cells/60 mm plate) in the presence of serum or in TGFβ1 under serum-free conditions. These findings are consistent with those reported previously in rabbits and humans.[2,5]

Immunohistochemical staining confirmed cell phenotypes via staining patterns of F-actin (Fig. 2) and α-SMA (Fig. 3). Keratocytes are quiescent cells not requiring a significant contractile

apparatus. Therefore, the presence of F-actin is less prominent and localized to the cortex of this cell type. Once activated, keratocytes can quickly develop higher levels of F-actin in an organized arrangement typical of their transformation into fibroblasts. The result is a morphological change from stellate to spindle shaped. F-actin staining in fibroblasts demonstrated an increase in F-actin which was more evenly distributed throughout the cytoplasm in visible bundles. Differentiation of myofibroblasts results in further cellular enlargement due to activation of protein synthesis and a greater increase in F-actin containing α-SMA, alpha-actinin and myosin. F-actin staining of myofibroblasts demonstrated prominent intra-cellular bundles indicative of a well-developed contractile apparatus. The increase in α-SMA yielded characteristic myofibroblast staining patterns not observed in either keratocyte or fibroblast cell culture populations.

This novel research model has similar benefits to other established *in vitro* models including: practicality, reproducibility, high proliferation rates, ability to control study environment, and the possibility of cell line cryopreservation. [21–23] Multiple *in vitro* and *in vivo* studies performed in experimental animals have significantly increased our understanding of cellular and molecular mechanisms involved in the development of corneal haze following keratitis. [17,22] Keratitis causes an alteration in the natural conformation of extracellular matrix and also changes the cellular density and phenotype of keratocytes.[17] These factors result in decreased corneal tissue transparency, commonly referred to as corneal haze.[22] The generation of corneal myofibroblast cells has recently been identified as the primary biological event responsible for the formation of corneal stromal opacification.[17,23–27] Myofibroblasts are highly contractile cells with increased backscattering of light attributable to decreased intracellular crystallin production.[27] Induction of myofibroblasts in corneal stroma plays a significant role in corneal fibrosis and long-term reduction in a clear visual axis.

In summary, the purpose of isolating and culturing equine corneal stromal fibroblasts, keratocytes, and myofibroblasts was to establish a reproducible *in vitro* model of pure cultures of these three cell types. This model will allow further investigation into the study of equine corneal wound healing. Investigations using anti-fibrotic agents and gene therapy are currently underway using this model.

Acknowledgments

Funding for this project was provided through RO1EY017294S1 (RRM) and RO1EY017294S2 (RRM) grants from the National Eye Institute, National Institutes of Health, Bethesda Maryland, Clinician Scientist Grant (EG, DB, RRM) from the University of Missouri, College of Veterinary Medicine, and an unrestricted grant from the Research to Prevent Blindness, New York, NY.

References

1. Barnett, K. Color Atlas and Text of Equine Ophthalmology. Mosby-Wolfe; Baltimore: 1995.
2. Gilger, BC. Equine Ophthalmology. Elsevier Saunders; St. Louis: 2005.
3. Gelatt, KN. Veterinary Ophthalmology. 4. Blackwell Publishing; Ames: 2007.
4. Jester JV, Barry-Lane PA, Cavanagh HD, et al. Induction of alpha-smooth muscle actin expression and myofibroblast transformation in cultured corneal keratocytes. Cornea 1996;15:505–516. [PubMed: 8862928]
5. Jester JV, Petroll WM, Cavanagh HD. Corneal stromal wound healing in refractive surgery: the role of myofibroblasts. Progress in Retinal and Eye Research 1999;18:311–356. [PubMed: 10192516]
6. Masur SK, Dewal HS, Dinh TT, et al. Myofibroblasts differentiate from fibroblasts when plated at low density. Proceedings of the National Academy of Sciences of the United States of America 1996;93:4219–4223. [PubMed: 8633044]

7. Wilson SE, Mohan RR, Ambrosio R Jr, et al. The corneal wound healing response: cytokine-mediated interaction of the epithelium, stroma, and inflammatory cells. Progress in Retinal Eye Research 2001;20:625–637.
8. Netto MV, Mohan RR, Sinha S, et al. Effect of prophylactic and therapeutic mitomycin C on corneal apoptosis, cellular proliferation, haze, and long-term keratocyte density in rabbits. Journal of Refractive Surgery 2006;22:562–574. [PubMed: 16805119]
9. Leccisotti A. Mitomycin C in photorefractive keratectomy: effect on epithelialization and predictability. Cornea 2008;27:288–291. [PubMed: 18362654]
10. Thornton I, Xu M, Krueger RR. Comparison of standard (0.02%) and low dose (0.002%) mitomycin C in the prevention of corneal haze following surface ablation for myopia. Journal of Refractive Surgery 2008;24:S68–S76. [PubMed: 18269154]
11. Shalaby A, Kaye GB, Gimbel HV. Mitomycin C in photorefractive keratectomy. Journal of Refractive Surgery 2009;25:S93–S97. [PubMed: 19248535]
12. Nassaralla BA, McLeod SD, Nassaralla JJ Jr. Prophylactic mitomycin C to inhibit corneal haze after photorefractive keratectomy for residual myopia following radial keratotomy. Journal of Refractive Surgery 2007;23:226–232. [PubMed: 17385287]
13. Srinivasan S, Drake A, Herzig S. Photorefractive keratectomy with 0.02% mitomycin C for treatment of residual refractive errors after LASIK. Journal of Refractive Surgery 2008;24:S64–S67. [PubMed: 18269153]
14. Sharma A, Mehan MM, Sinha S, et al. Trichostatin A inhibits corneal haze *in vitro* and *in vivo*. Investigative Ophthalmology and Visual Science 2009;50:2695–2701. [PubMed: 19168895]
15. Mohan RR, Stapleton WM, Sinha S, et al. Decorin gene transfer into keratocytes inhibits alpha smooth muscle actin (SMA) expression and myofibroblast transformation. Investigative Ophthalmology & Visual Science 2006;47:E 1815.
16. Barnett, KC. Equine Ophthalmology: An Atlas and Text. 2. Saunders; Edinburgh; New York: 2004.
17. Haber M, Cao Z, Panjwani N, et al. Effects of growth factors (EGF, PDGF-BB and TGF-beta 1) on cultured equine epithelial cells and keratocytes: implications for wound healing. Veterinary Ophthalmology 2003;6:211–217. [PubMed: 12950652]
18. Hong JW, Liu JJ, Lee JS, et al. Proinflammatory chemokine induction in keratocytes and inflammatory cell infiltration into the cornea. Investigative Ophthalmology and Visual Science 2001;42:2795–2803. [PubMed: 11687520]
19. Masur SK, Cheung JK, Antohi S. Identification of integrins in cultured corneal fibroblasts and in isolated keratocytes. Investigative Ophthalmology and Visual Science 1993;34:2690–2698. [PubMed: 8344791]
20. Werner A, Braun M, Reichl S, et al. Establishing and functional testing of a canine corneal construct. Veterinary Ophthalmology 2008;11:280–289. [PubMed: 19046287]
21. Werner A, Braun M, Kietzmann M. Isolation and cultivation of canine corneal cells for *in vitro* studies on the anti-inflammatory effects of dexamethasone. Veterinary Ophthalmology 2008;11:67–74. [PubMed: 18302570]
22. Toropainen E, Ranta VP, Talvitie A, et al. Culture model of human corneal epithelium for prediction of ocular drug absorption. Investigative Ophthalmology and Visual Science 2001;42:2942–2948. [PubMed: 11687540]
23. Tegtmeyer S, Reichl S, Muller-Goymann CC. Cultivation and characterization of a bovine *in vitro* model of the cornea. Pharmazie 2004;59:464–471. [PubMed: 15248462]
24. Netto MV, Mohan RR, Ambrosio R Jr, et al. Wound healing in the cornea: a review of refractive surgery complications and new prospects for therapy. Cornea 2005;24:509–522. [PubMed: 15968154]
25. Netto MV, Mohan RR, Sinha S, et al. Stromal haze, myofibroblasts, and surface irregularity after PRK. Experimental Eye Research 2006;82:788–797. [PubMed: 16303127]
26. Mohan RR, Hutcheon AE, Choi R, et al. Apoptosis, necrosis, proliferation, and myofibroblast generation in the stroma following LASIK and PRK. Experimental Eye Research 2003;76:71–87. [PubMed: 12589777]
27. Jester JV, Moller-Pedersen T, Huang J, et al. The cellular basis of corneal transparency: evidence for 'corneal crystallins'. Journal of Cell Science 1999;112(Pt 5):613–622. [PubMed: 9973596]

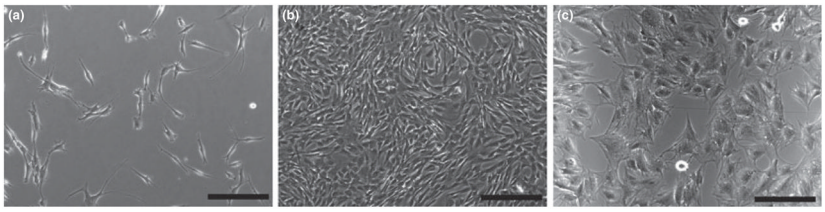

Figure 1.
Light microscopy phase-contrast images of (a) keratocytes demonstrating broad, stellate cytoplasmic morphology with multiple interconnected cellular processes, (b) fibroblasts demonstrated a classic spindle shaped morphology, as did (c) myofibroblasts; however, this phenotype was larger in overall size due to the developed contractile apparatus. Calibration bar = 100 μm.

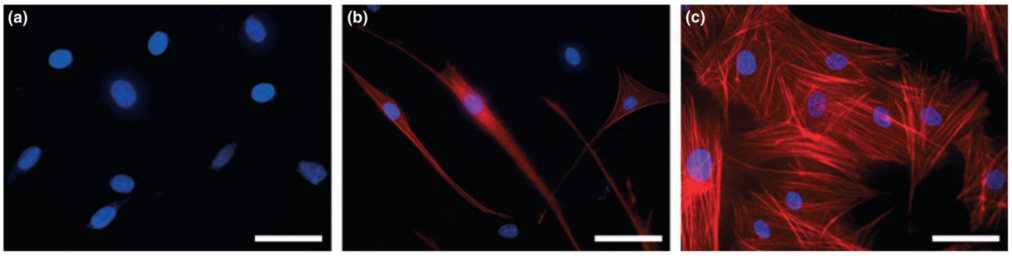

Figure 2.
Immunocytochemical staining with phalloidin (red) showing expression and localization of F-actin in equine keratocytes, fibroblasts and myofibroblasts. Nuclei are stained blue by DAPI. Keratocytes (a) demonstrated no positive F-actin staining. Fibroblasts (b) were spindle shaped with intracellular F-actin bundles. Myofibroblasts (c) demonstrated strong F-actin staining showing prominent microfilament apparatus. Bar = 100 μm.

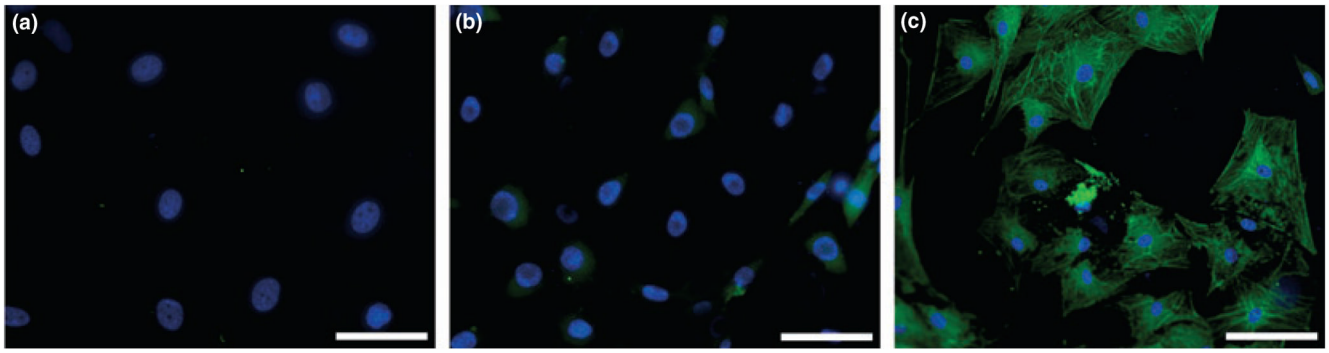

Figure 3.
Immunocytochemical staining showing expression and localization of α-SMA (green) in equine keratocytes, fibroblasts and myofibroblasts. Nuclei are stained blue by DAPI. Negative staining in keratocytes (a), sparsely positive in fibroblasts (b) and abundantly positive in myofibroblasts (c). Bar = 100 μm.

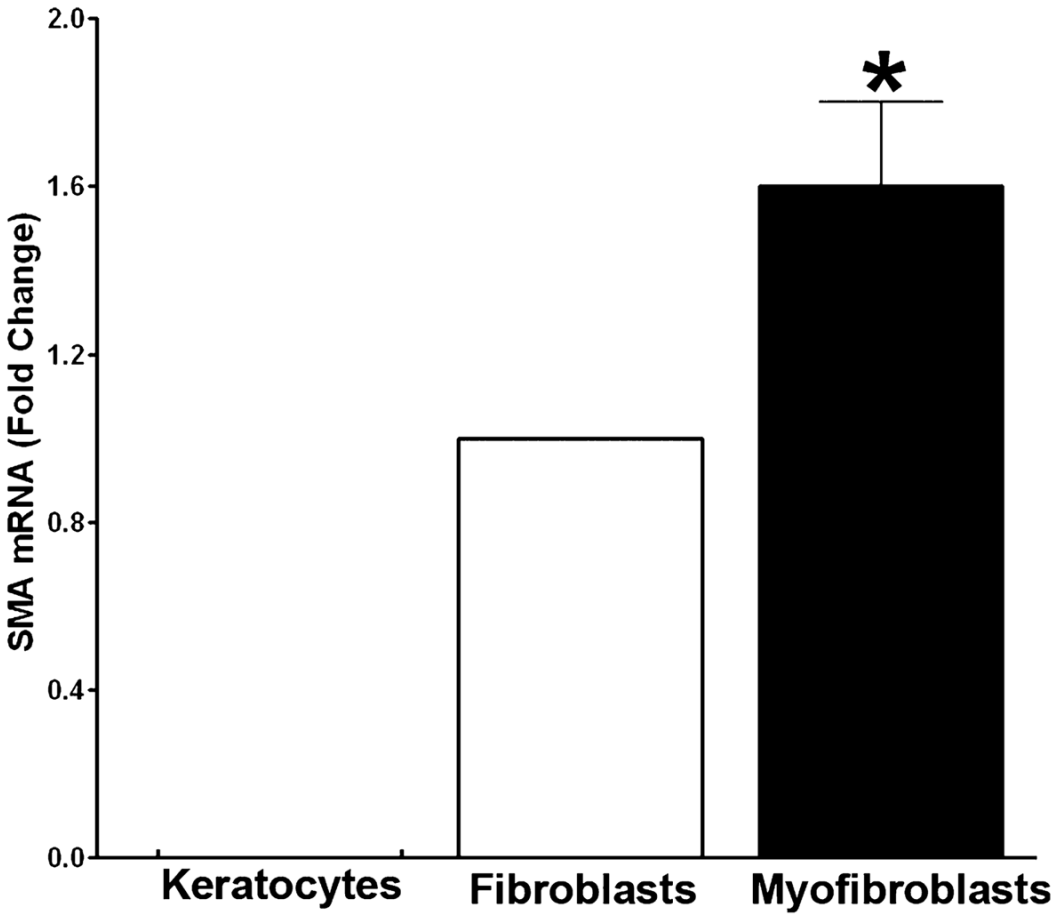

Figure 4.

Real-time graph demonstrating the results of quantitative real-time PCR measurements of α-SMA in equine keratocytes, fibroblasts and myofibroblasts. A statistically significant increase in α-SMA was noted in myofibroblasts compared to keratocytes and fibroblasts. The asterisk indicates a $P < 0.01$.